

# Novel polymer inclusion membrane containing a macrocyclic ionophore for selective removal of strontium from nuclear waste solution†

Prasanta K. Mohapatra, Priyanath N. Pathak, Anup Kelkar‡ and Vijay K. Manchanda\*

Radiochemistry Division, B.A.R.C., Trombay, Mumbai 400085, India.

E-mail: acsred@magnum.barc.ernet.in; Fax: +91-22-25505151

Received (in Montpellier, France) 23rd May 2003, Accepted 24th February 2004

First published as an Advance Article on the web 9th July 2004

A new polymer inclusion membrane (PIM) containing cellulose triacetate (CTA) as the monomer, di-*tert*-butylcyclohexano-18-crown-6 (DtBuCH18C6) as the carrier and 2-nitrophenyl octyl ether (NPOE) as the plasticizer was developed for the selective transport of  $\text{Sr}^{2+}$  from aqueous nitrate medium. Studies with crown ether concentration variation have indicated a linear dependence on the permeability coefficient ( $P$ ) suggesting a diffusion mechanism for ion transport. Effects of membrane thickness, nature of plasticizer and plasticizer concentration on the transport of  $\text{Sr}^{2+}$  were studied. The effect of feed acidity was also investigated for a possible application in the nuclear waste solution. Selective  $\text{Sr}^{2+}$  transport was observed in a synthetic waste solution containing metal ions such as  $\text{UO}_2^{2+}$ ,  $\text{MoO}_2^{2+}$ ,  $\text{Zr}^{4+}$ ,  $\text{Ce}^{3+}$ ,  $\text{Nd}^{3+}$ ,  $\text{Ru}^{3+}$ ,  $\text{Pd}^{2+}$ ,  $\text{Ba}^{2+}$  and  $\text{Cs}^+$ , *etc.*, in 1 M  $\text{HNO}_3$  and 2 M  $\text{NaNO}_3$ . Greater than 70% transport of  $\text{Sr}^{2+}$  was observed in 24 h while most of the other metal ions were negligibly transported (<0.01%).

## Introduction

Due to growing concerns for environment protection, radioactive waste management has emerged as one of the most challenging areas of present day research.  $^{90}\text{Sr}$  ( $t_{1/2} = 28.5$  years) is one of the most important fission products present in high level waste (HLW) solution generated during the reprocessing of spent nuclear fuel. The separation of long lived  $^{90}\text{Sr}$  from HLW prior to vitrification is helpful not only to reduce the volume of disposable waste but also reduces the risk of matrix deformation caused by the generated heat.<sup>1</sup> In addition, the separated radionuclide has many applications, *viz.* as a fuel for thermoelectric and thermomechanical power generators (RTGs and RTMGs).

For the separation of Sr from acidic nitrate medium (HLW usually contains 1–3 M nitric acid), several methods like precipitation, ion exchange and solvent extraction have been reported.<sup>2</sup> Out of these, solvent extraction methods with crown ether ligands are particularly exciting due to their ease of operation and specificity. Horwitz *et al.*<sup>3–5</sup> have developed the SREX process using one such substituted crown ether, the *t*-butyl derivative of dicyclohexano-18-crown-6, in octanol as the diluent. As the reagent is particularly expensive, any plant scale application requires suitable modifications to reduce the ligand inventory to make the process cost effective.

Using a more polar diluent mixture, such as 80% butanol and 20% octanol, the ligand inventory can be reduced.<sup>6</sup> However, significant reduction in the ligand inventory can also be achieved by using a membrane-based separation method.<sup>7–10</sup>

In recent years, separation methods based on polymeric inclusion membranes (PIMs) have received considerable attention due to the high stability of such membranes compared to that of supported liquid membranes.<sup>11</sup> PIMs consist of (i) cellulose triacetate (CTA) as the polymer support, (ii) a carrier ligand for cation transport and (iii) a liquid plasticizer that acts as an organic solvent similar to that used in liquid-liquid extraction systems. For selective transport, crown ethers have been found to be particularly useful carriers.<sup>12</sup>

The present work deals with the evaluation of several PIMs, incorporating various macrocyclic carriers [*viz.* dibenzo-18-crown-6 (DB18C6), *cis*-dicyclohexano-18-crown-6 (*cis*-DCH18C6), dicyclohexano-18-crown-6 (DCH18C6) and di-*tert*-butylcyclohexano-18-crown-6 (DtBuCH18C6; shown in Chart 1)] and plasticizers [*viz.* 2-nitrophenyl-*n*-octyl ether (NPOE), tris(2-ethylhexyl) phosphate (TEHP), tri-*n*-butyl phosphate (TBP)] for the selective transport of  $\text{Sr}^{2+}$ . The best results have been obtained when DtBuCH18C6 and NPOE were used as carrier and plasticizer, respectively. Therefore, all subsequent studies have been carried out using the membranes cast from CTA, DtBuCH18C6 and NPOE. The effect of various other factors such as the nature of the crown ether, crown ether concentration, nature of plasticizer, plasticizer

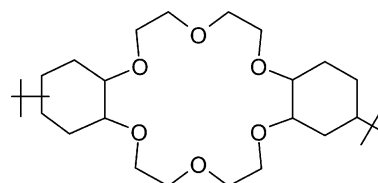


**Chart 1** Structure of di-*tert*-butylcyclohexano-18-crown-6 (DtBuCH18C6).

† Abbreviations: CTA = cellulose triacetate, PIM = polymer inclusion membrane, SLM = supported liquid membrane, HPGe = high purity germanium, HLW = high level waste, SHLW = simulated high level waste, HWR = pressurized heavy water reactor, DCH18C6 = dicyclohexano-18-crown-6, DtBuCH18C6 = di-*t*-butylcyclohexano-18-crown-6, NPOE = 2-nitrophenyl octyl ether, TBP = tri-*n*-butyl phosphate, TEHP = tris(2-ethyl hexyl) phosphate. Symbols:  $D_m$  = diffusion coefficient of the complex,  $d_m$  = membrane thickness,  $C_{mf}$  = Sr concentration at the membrane feed interface,  $C_{mr}$  = Sr concentration at the membrane receiver interface,  $P$  = permeability coefficient,  $J$  = flux,  $k$  = Boltzmann constant,  $\eta$  = viscosity.

‡ Present address: Advanced Fuel Fabrication Facility, Nuclear Fuels Group, B.A.R.C., Tarapur, Maharashtra 401502, India

concentration, membrane thickness, nature and concentration of foreign cations, feed acidity, proton transport across the PIM, acid uptake by the PIM,  $\text{NO}_3^-$  ion concentration, *etc.*, on the cation transport has also been investigated. The transport behaviour of Sr in simulated high level nuclear waste has also been studied. Finally, the selective transport of Sr from a host of fission products, obtained from an irradiated natural uranium target has been studied.

## Experimental

### Materials

DCH18C6 (Aldrich), *cis*-DCH18C6 (Aldrich), DB18C6 (Merck), DtBuCH18C6 (Fluka) and NPOE (Fluka) were used as procured. CTA was obtained from Alfa Biochem.  $^{85,89}\text{Sr}$  tracer was from BRIT, Mumbai. All other reagents were of AR grade.

### Preparation and characterization of CTA membrane

The PIMs were prepared using the method reported by Lamb and Nazarenko.<sup>13</sup> For example, 5 mL of chloroform solution containing  $12.5 \text{ mg cm}^{-3}$  CTA,  $6 \text{ mg cm}^{-3}$  of DtBuCH18C6 and 0.1 mL NPOE were cast in a glass culture dish (flat bottom, 9 cm diameter) after thorough mixing (sonification). Following evaporation of the solvent and setting of the CTA membrane,  $\sim 1 \text{ mL}$  of water was swirled on top of the film to help loosen it from the glass. The polymer film was then carefully peeled out from the dish. The resulting membrane contained 37.7 wt % CTA, 13.8 wt % DtBuCH18C6 and 48.5% NPOE. Membranes with different concentrations of crown ether, plasticizer and CTA were prepared in a similar fashion.

The thickness of the membranes was measured with a Mitutoyo Digital micrometer. The thickness was also calculated from weight per  $\text{cm}^{-2}$  measurements. Both the values agreed within error limits ( $\pm 5\%$ ).

The acid uptake by the PIM was measured using  $1 \text{ cm}^2$  pieces of different portions of the membrane, which were soaked in 3 M  $\text{HNO}_3$  and continuously stirred for 2 h. The acid-soaked membranes were dried and dissolved in  $\text{CHCl}_3$  and stored overnight. The absorbed nitric acid was stripped using 10 mL distilled water. A known aliquot of this aqueous phase was titrated with standard NaOH solution using phenolphthalein as indicator.

The amount of nitric acid transported through the PIM was determined volumetrically. A known aliquot of the receiver phase was titrated with standard NaOH using phenolphthalein as the indicator.

### Membrane transport experiments

The apparatus used for the transport experiment was a permeability cell consisting of two cylindrical glass compartments separated by a membrane. The half cell volumes were 24 mL each and the effective membrane area was  $4.94 \text{ cm}^2$ . The CTA membrane was fixed between the two compartments of the cell using metallic clips. The feed (source) compartment or the source phase usually contained  $\text{NO}_3^-$  ion while distilled water was used as the stripper in the receiver compartment. The side of the film exposed to air during evaporation was placed so as to face the vessel containing the source solution.<sup>14</sup> Equal volumes of source and receiver phase were transferred into the respective compartments and the source phase was spiked with  $^{85,89}\text{Sr}$  tracer. Both sides were stirred with Teflon-coated magnetic stirring bars at 250 rpm by synchronous motors. Samples (0.1 mL) from both the feed and receiver were

periodically taken out and assayed radiometrically (514 keV gamma line) using a well-type NaI(Tl) scintillation counter.

**Studies with simulated high level waste (SHLW) solution.** SHLW solution (PHWR type) was prepared by dissolving the various constituents as desired (Table 1).<sup>15</sup> Nitrate salts were preferred for this preparation. The experiment with the simulated waste solution contained 1 M  $\text{HNO}_3$  + 2 M  $\text{NaNO}_3$ .

**Studies with irradiated natural uranium target.** Transport selectivity of the present PIM for  $\text{Sr}^{2+}$  with respect to other fission products was investigated by irradiating a natural uranium target ( $\sim 2 \text{ mg}$ ) wrapped with Al foil at a thermal neutron flux of  $1 \times 10^{12} \text{ neutron cm}^{-2} \text{ s}^{-1}$ . Subsequently, the Al foil containing the fission products was dissolved in concentrated HCl and converted to nitrate form by repeated evaporation to dryness using a few drops of concentrated  $\text{HNO}_3$ . Finally, the medium was adjusted to 1 M  $\text{HNO}_3$  + 2 M  $\text{NaNO}_3$ . The gamma spectrum was recorded by an HPGe detector connected to a multichannel analyzer.

## Results and discussion

### Separation of metal ions by PIMs

Eighteen-membered crown ethers (cavity radius =  $1.45 \pm 0.15 \text{ \AA}$ ) were found to favourably extract  $\text{Ba}^{2+}$  (ionic radius =  $1.35 \text{ \AA}$ ) as compared to  $\text{Sr}^{2+}$  (ionic radius =  $1.13 \text{ \AA}$ ) from aqueous picrate medium, which was explained on the basis of the size selective complexation property of these crown ethers.<sup>16</sup> From nitric acid medium, however, an opposite trend was observed by Horwitz *et al.*,<sup>3</sup> which was attributed to an entirely different extraction mechanism with the extracted species reportedly containing water molecules and nitrate ions. Previous studies with the supported liquid membrane system (SLM) containing DtBuCH18C6 in *n*-octanol as the carrier indicated significant transport of  $\text{Sr}^{2+}$  from nitrate medium, the main constraint being the stability of the membrane.<sup>12,17</sup> It was logical, therefore, to develop a PIM (which has significantly higher stability as compared to SLMs) containing the crown ether for  $\text{Sr}^{2+}$  permeation.

Separation of metal ions by PIMs consists of the following three steps, *viz.* complex formation of metal ion with the

**Table 1** Composition of simulated high level waste (SHLW) for a pressurised heavy water reactor (PHWR) ( $\sim 6000 \text{ MW day/tonne}$ )

Constituent	Concentration/ $\text{mg dm}^{-3}$	Constituent	Concentration/ $\text{mg dm}^{-3}$
$\text{Sr}^a$	186.3	$\text{Sb}^b$	4.7
$\text{Rb}^a$	74.5	$\text{Se}^b$	12.3
$\text{Zr}^a$	771.3	$\text{Dy}^c$	2.0
$\text{Ag}^a$	18.6	$\text{Sn}^b$	15.6
$\text{Ba}^a$	308.8	$\text{Te}^b$	102.8
$\text{Cd}^a$	16.3	$\text{Sm}^c$	163.8
$\text{Ce}^a$	532.5	$\text{Tb}^c$	5.0
$\text{Cs}^a$	543.8	$\text{Gd}^c$	165
$\text{Fe}^a$	500	$\text{Eu}^c$	22.6
$\text{Cr}^a$	100	$\text{Pr}^c$	243.8
$\text{Co}^{a,e}$	127.5	$\text{Nd}^c$	862.5
$\text{Na}^a$	3000	$\text{La}^{c,f}$	263.8
$\text{Ni}^a$	100	$\text{Pd}^d$	267.5
$\text{U}^a$	18325	$\text{Ru}^d$	463.8
$\text{Mn}^{a,g}$	181.3	$\text{Y}^d$	99
$\text{Mo}^b$	731.3		

<sup>a</sup> Nitrate salt. <sup>b</sup> Metal powder. <sup>c</sup> Oxide. <sup>d</sup> Chloride salt. <sup>e</sup> Taken in place of Rh. <sup>f</sup> Taken in place of Pm. <sup>g</sup> Taken in place of Tc.

extractant at the feed side of membrane (feed–membrane interface), diffusion of the complexed species to the opposite side of the membrane and liberation of the metal ion at the receiver side of the membrane (membrane–receiver interface). However, the transfer of such species across the interface necessitates the presence of a suitable counteranion in the source (feed) phase.

Assuming that the transport of metal ions occurs at steady state and that the concentration gradients are linear, the flux ( $J$ ) is given by an appropriate formulation of Fick's first law of diffusion:

$$J = D_m(C_{mf} - C_{mr})/d_m \quad (1)$$

where  $D_m$  is the diffusion coefficient of the complex,  $d_m$  is the membrane thickness,  $C_{mf}$  and  $C_{mr}$  are the concentrations of metal ion at the membrane–feed interface and membrane–receiver interface, respectively. Under efficient stripping conditions ( $C_{mf} \gg C_{mr}$ ) and neglecting the aqueous diffusion layer ( $C_{mf} \sim C_f$ ), eqn. (1) is simplified to:

$$P = J/C_f \quad (2)$$

where  $C_f$  is the bulk concentration of metal ion in the feed and  $P$  is the permeability coefficient.  $P$  can be obtained using the following equation:

$$\ln(C_{f,t}/C_{f,0}) = -(Q/V)Pt \quad (3)$$

where  $C_{f,t}$  and  $C_{f,0}$  are the concentrations of metal ion in the aqueous feed at time  $t$  and at  $t = 0$ , respectively,  $Q$  is the surface area and  $V$  is the aqueous feed volume (in mL).

### Transport of $\text{Sr}^{2+}$

**The effect of the nature of ligand.** Though it was decided to employ 18-membered crown ethers for  $\text{Sr}^{2+}$  transport, the role of substituents, which affect the lipophilicity and basicity of the ligand and also the mobility of the complex, was investigated. Table 2 shows that transport of  $\text{Sr}^{2+}$  is poor (<1%) for all the 18-membered crown ether ligands other than DtBuCH18C6, for which about 35% transport through the PIM was observed after 6 h. The higher transport rate observed for DtBuCH18C6 has been attributed to (i) the existence of this ligand as a monomer over a wide concentration range as compared to the aggregation of DCH18C6 above 0.01 M,<sup>3</sup> (ii) the increase in the electron density on the crown ether ring oxygens due to the +I effect of *t*-butyl group in DtBuCH18C6 and (iii) the steric effect of the *t*-butyl group.

**The effect of crown ether concentration.** In an attempt to elucidate the PIM transport mechanism, experiments were designed to establish the relationship between ligand concentration in the membrane and the transport of  $\text{Sr}^{2+}$  ion. The crown ether content in the membrane was varied from 1.7 to 30 mM. However, as the increase in ligand concentration resulted in increased thickness of the membranes (which affects the transport rates), the ligand concentration was restricted to 30 mM. As shown in Fig. 1, the permeability coefficient ( $P$ )

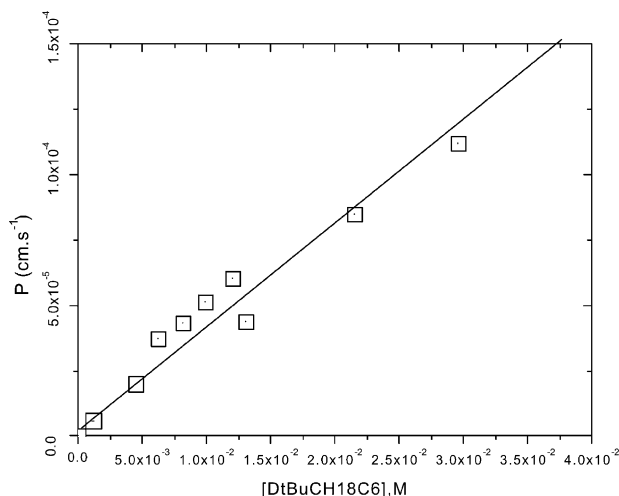


**Fig. 1** Variation of the permeability coefficient ( $P$ ) with DtBuCH18C6 concentration in the PIM [feed: 3 M  $\text{NaNO}_3$  containing  $^{85,89}\text{Sr}$  tracer ( $\sim 10^{-5}$  M); receiver: distilled water].

values vary linearly and a slight decrease is observed at higher ligand concentration. This result is consistent with a diffusion-based transport mechanism for the SLMs as described by McBride *et al.*<sup>18</sup> Diffusion-based transport involves complex formation of the metal ion at the surface of PIM, followed by diffusion of the entire complex to the opposite side of the PIM and finally liberation of the metal at the opposite interface (Fig. 2). On the other hand, for a site-jumping mechanism to be operative, in which the metal ion jumps from one ligand moiety to the other, a breakthrough ligand concentration is required before the  $P$  is measurable.<sup>19</sup>

**The role of plasticizer.** To study the role of the plasticizer in the transport of  $\text{Sr}^{2+}$ , membranes were prepared using different plasticizers: NPOE, tris(2-ethylhexyl) phosphate (TEHP) and tri-*n*-butyl phosphate (TBP). Transport of  $\text{Sr}^{2+}$  from a feed of 3 M  $\text{NaNO}_3$  was monitored for 20 h using membranes made from various plasticizers and the measured  $P$  values are listed in Table 3. Upon increasing the plasticizer concentration by 2, the  $P$  value doubled, suggesting the importance of the plasticizer in the preparation of the membrane. As seen from Table 3, TBP gave a marginally higher transport rate as compared to NPOE, while TEHP gave quite inferior results. Although the transport rate was highest for TBP, it has poor selectivity as many other metal ions could also be transported.<sup>20</sup> It is reported that TBP forms solvated species such as  $\text{M}(\text{NO}_3)_n \cdot m\text{TBP}$  that are responsible for metal ion extraction. Metal ions such as  $\text{Zr}^{4+}$ ,  $\text{MoO}_2^{2+}$  and  $\text{Ru}^{3+}$  could, therefore, be extracted as their solvated complexes. On the other hand, no such solvation properties are known for NPOE and all the subsequent experiments were, therefore, carried out using membranes made with NPOE.

The diffusion coefficient of the complex in the membrane is inversely proportional to the viscosity of the membrane

**Table 2** Transport of Sr through PIMs with different 18-membered crown ethers<sup>a</sup>

Crown ether	% Sr transport
DB18C6	0.3
DCH18C6	0.6
<i>cis</i> -DCH18C6	0.7
DtBuCH18C6	35

<sup>a</sup> Crown ether: 0.2 M; feed: 3 M  $\text{NaNO}_3$  containing  $^{85,89}\text{Sr}$  tracer ( $\sim 10^{-5}$  M); stripping phase: distilled water; duration: 6 h.

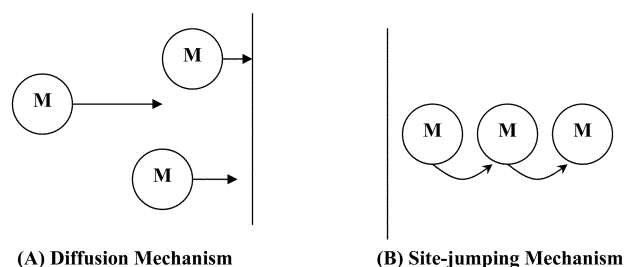


**Fig. 2** Proposed models of Sr transport.

**Table 3** Physical parameters of different plasticizers and the permeability coefficients through the PIMs<sup>a</sup>

Plasticizer	Plasticizer amount/ $\mu\text{L}$	$10^5 P/\text{cm s}^{-1}$	Viscosity/cP	Dielectric constant
NPOE	100	5.8	13.8	24
NPOE	200	11.7	13.8	24
TEHP	200	1.1	10.2	—
TBP	200	14	3.32	8.09

<sup>a</sup> Feed: 3 M  $\text{NaNO}_3$  containing  $^{85,89}\text{Sr}$  tracer ( $\sim 10^{-5}$  M); stripping phase: distilled water; duration: 20 h.

phase,  $\eta$ , if it follows the Stokes–Einstein equation:

$$D = kT/6\pi r\eta \quad (4)$$

where  $k$  is the Boltzmann constant,  $T$  is the absolute temperature and  $r$  is the molecular radius of the complex. Table 3 lists the values of viscosity and dielectric constants of the plasticizers used in the present work. The diffusion of the complex in the membrane is mainly governed by the polarity of the plasticizer and probably depends to lesser extent on the viscosity.

**Effect of NPOE concentration on Sr transport rate.** As shown in Table 3, the plasticizer concentration has a direct effect on the transport rate. In a detailed investigation, the plasticizer content in the membrane was varied from 33.1 wt % to 64.9 wt %. As seen in Fig. 3, transport is highest for the membrane having the highest amount of NPOE, which suggests that the fluid content in the membrane determines the transport of Sr. The ratio of CTA and NPOE is critical for metal ion transport. Higher CTA (or lower NPOE) concentrations decrease transport due to greater resistance by the polymer framework. On the other hand, a greater plasticizer fraction can enhance transport due to less obstruction and high fluid content in the membrane phase.

**The effect of thickness of the membrane.** As per eqn. (1), the transport rate is inversely proportional to the thickness of the membrane. Several membranes with varying thicknesses were

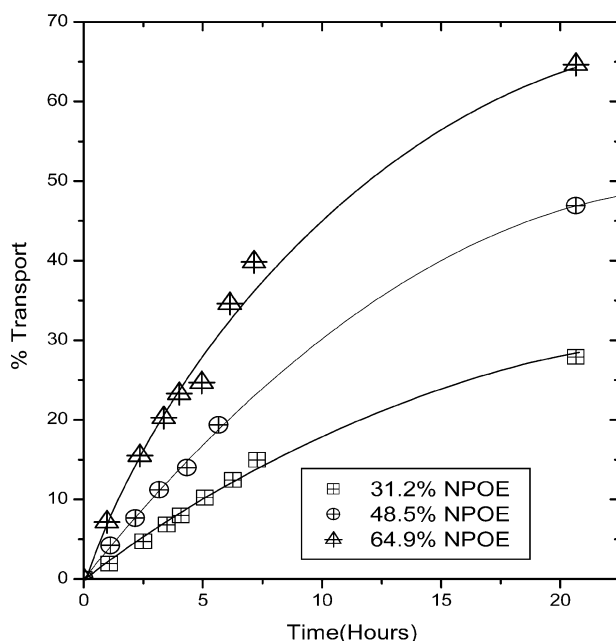


**Fig. 3** Variation of Sr transport with plasticizer concentration in the PIM [feed: 3 M  $\text{NaNO}_3$  containing  $^{85,89}\text{Sr}$  tracer ( $\sim 10^{-5}$  M); receiver: distilled water].

**Table 4** Sr transport as a function of the membrane thickness<sup>a</sup>

CTA	Membrane thickness/ $\mu\text{m}$	% Sr transport	$10^5 P/\text{cm s}^{-1}$
23.4%	23.6	80.7	14
37.7%	27	46.9	4.9
47.6%	29	42.4	4.2

<sup>a</sup> Feed: 3 M  $\text{NaNO}_3$  containing  $^{85,89}\text{Sr}$  tracer ( $\sim 10^{-5}$  M); stripping phase: distilled water. Duration 20 h.

prepared and the permeability coefficients were measured. The standard aliquot of CTA in chloroform used to prepare the PIMs was 5 mL of a  $12.5 \text{ mg mL}^{-1}$  CTA solution that, once polymerized generated a membrane of  $27.0 \mu\text{m}$  thickness. Membranes were also prepared with varying amounts of CTA, which yielded membranes with different thicknesses; the corresponding transport rates were measured. Table 4 shows the effect of membrane thickness on the transport and permeability. As expected, larger amounts of CTA generated thicker, stronger membranes with decreased transport properties. Use of less CTA resulted in a thinner membrane with increased transport and permeability but that suffered from a greater fragility. From this experiment, the optimum proportion of CTA was taken as 37% for further experiments.

**Optimization of membrane parameters.** From the above discussion, it is clear that the  $\text{Sr}^{2+}$  transport rate depends directly on the crown ether concentration, NPOE concentration and inversely on the CTA concentration. Increasing the concentration of all three components increased the thickness of the membrane, which decreased the transport rates. Though thinner membranes showed higher transport rates their mechanical stability was poor. Based on all these considerations, the optimum concentrations of the three components for subsequent experiments were fixed at 37.7 wt % CTA, 13.8 wt % DtBuCH18C6 and 48.5 wt % NPOE.

**Effect of feed acidity.** High level nuclear waste (HLW) solutions usually contain nitric acid in the concentration range of 1–3 M. It was of interest, therefore, to investigate the transport rates as a function of nitric acid concentration, fixing or not the total nitrate concentration.<sup>21</sup> Transport of  $\text{Sr}^{2+}$  was investigated as a function of feed nitric acid concentration and the permeability coefficients are given in Table 5. The transport rate is much higher as compared to 3 M  $\text{NaNO}_3$  medium. But the membrane is less stable in 3 M nitric acid medium. This could be due to acid hydrolysis of the CTA membrane. To prove this point, acid transport across the membrane and acid uptake by the membrane were measured. It was found that apart from Sr transport, protons were also transported across the membrane. The transport of protons in 2 and 3 M nitric acid feed is quite significant and is the likely reason for the lower than expected flux in this system.<sup>21</sup>

**Table 5** Transport properties and permeability coefficient of the PIM as a function of the feed acidity<sup>a</sup>

$\text{HNO}_3/\text{M}$	% Sr transport	$10^5 P/\text{cm s}^{-1}$	% Acid transport
1	15.8	4.6	1.1
2	23.9	15	4.2
3	43.7	17	6.6

<sup>a</sup> Feed: nitric acid solution of variable concentration (1–3 M) containing  $^{85,89}\text{Sr}$  tracer ( $\sim 10^{-5}$  M); stripping phase: distilled water; duration: 4 h.



**Table 6** Amount of acid absorbed as a function of the thickness of the PIM when dipped in 3 M HNO<sub>3</sub> for 2 h

PIM composition			Thickness/ μm	Acid uptake/ mol cm <sup>-2</sup>
% CTA	% DtBuCH18C6	% NPOE		
23.4	17	59.6	23.6	0.002
47.6	11.9	40.5	25	0.02
49.8	18.5	31.7	29.2	0.04

Table 6 shows the amount of acid absorbed by the membrane during a 2 h exposure to 3 M nitric acid medium. The amount of acid absorbed by the membrane increases with the increase in CTA content in the membrane. These results show that at higher feed acidity the CTA matrix is hydrolyzed after absorption of acid by the membrane, thus destabilizing it. Due to the instability of the membrane at 3 M HNO<sub>3</sub> further transport studies has been carried out in 1 M HNO<sub>3</sub> + 2 M NaNO<sub>3</sub>.

**Transport behaviour of Sr in simulated waste.** Table 1 shows the composition of the simulated waste and Fig. 4 depicts the transport of Sr<sup>2+</sup> in a simulated waste solution prepared in 1 M HNO<sub>3</sub> + 2 M NaNO<sub>3</sub>. Here the transport of Sr<sup>2+</sup> is much lower as compared to that obtained with pure 1 M HNO<sub>3</sub> + 2 M NaNO<sub>3</sub>. After 12 h stirring the receiver phase became pale yellow, which indicates that some other metal ions are also competing with Sr transport. It appears that metal ions other than Sr<sup>2+</sup> may be forming extractable complexes with the crown ether at the feed-membrane interface but may not get stripped in the receiver phase, thereby affecting the free crown ether concentration and resulting in a low permeability coefficient value for Sr<sup>2+</sup>.

**Selective transport of Sr.** The transport selectivity of the present PIM for Sr<sup>2+</sup> with respect to other fission products was investigated by irradiating a natural uranium target wrapped in Al foil with a thermal neutron flux. Subsequently, the Al foil containing the fission products was dissolved in 1 M HNO<sub>3</sub>, the solution was evaporated to dryness and finally dissolved in 1 M HNO<sub>3</sub> + 2 M NaNO<sub>3</sub>. The fission product mixture

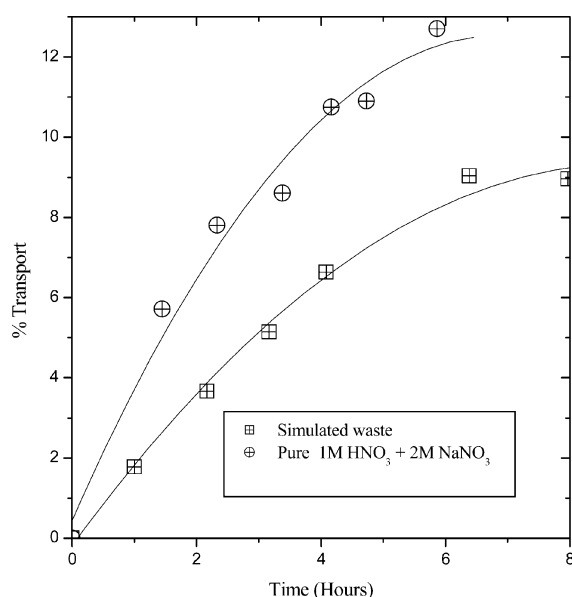


**Fig. 4** Transport behaviour of Sr in the presence and absence of simulated waste (feed solution: <sup>85,89</sup>Sr tracer in 1 M HNO<sub>3</sub> + 2 M NaNO<sub>3</sub> without/with simulated waste; receiver: distilled water).

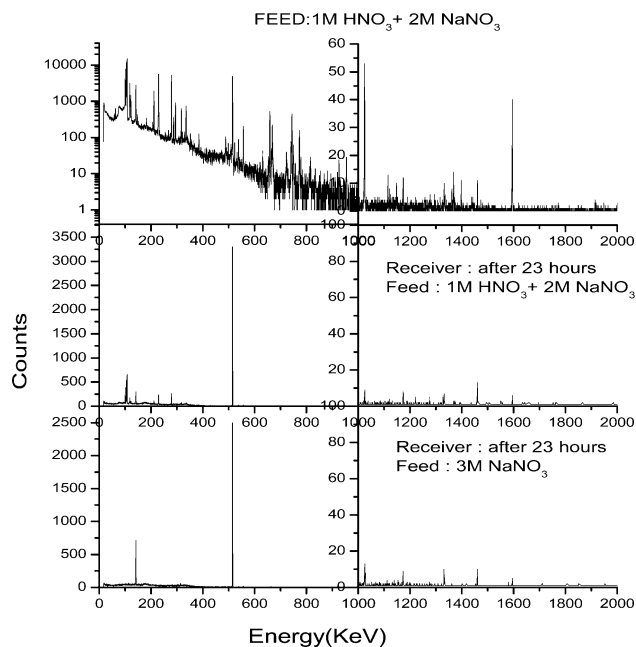


**Fig. 5** Gamma spectrum of an irradiated uranium solution spiked with <sup>85,89</sup>Sr tracer ( $\sim 10^{-5}$  M) in 1 M HNO<sub>3</sub> + 2 M NaNO<sub>3</sub> showing selective transport of Sr across the PIM (receiver: distilled water; duration: 23 h).

was spiked with <sup>85,89</sup>Sr tracer as these nuclides are not formed to any significant extent during the short irradiation period employed. The transport of various fission products was monitored at the end of 23 h. Fig. 5 shows the recorded gamma spectrum, which clearly suggests that Sr<sup>2+</sup> (as indicated by the 514 keV gamma line) is selectively transported as compared to other nuclides, including <sup>96</sup>Nb, <sup>97</sup>Zr, <sup>99</sup>Mo, <sup>103</sup>Ru, <sup>143</sup>Ce and <sup>151</sup>Pm. Interference of <sup>140</sup>Ba (8.4% transport) is explained on the basis of the size of Ba<sup>2+</sup> (1.35 Å), which matches with the cavity size of the 18-membered ligand. The significantly larger Sr<sup>2+</sup> transport compared to the data obtained with pure 1 M HNO<sub>3</sub> + 2 M NaNO<sub>3</sub> is attributed to the presence of Al(NO<sub>3</sub>)<sub>3</sub>, which has a greater salting out effect as compared to NaNO<sub>3</sub> alone.

**Stability of the PIM.** A transport experiment with 30 μm thick PIM, containing 1 M HNO<sub>3</sub> + 2 M NaNO<sub>3</sub> as feed solution and distilled water as receiver phase, was allowed to run for 15 days. No significant variation in Sr transport behaviour was observed (Fig. 6). The membrane recovered from this

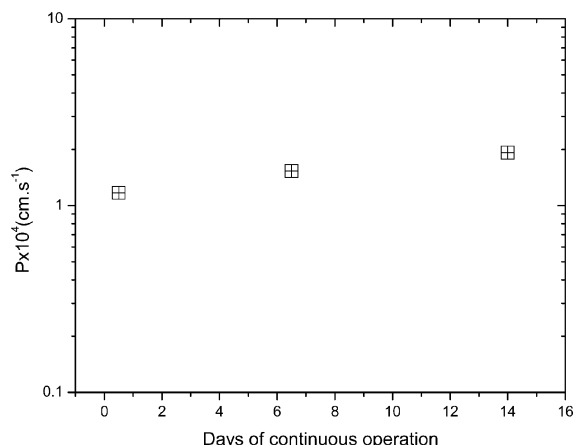


**Fig. 6** Stability of the PIM as a function of time [feed: <sup>85,89</sup>Sr tracer ( $\sim 10^{-5}$  M) in 1 M HNO<sub>3</sub> + 2 M NaNO<sub>3</sub>; receiver: distilled water].

experiment was physically intact, showing no evidence of deterioration after extended use. The marginal increase in the  $P$  values was a result of a slight decrease in the thickness of the membrane due to continuous operation. In the presence of 3 M  $\text{HNO}_3$ , the membrane was no longer stable after 12 h of use (*vide supra*).

## Conclusions

The polymer inclusion membrane entraps macrocyclic carriers in the membrane matrix during the casting process, effectively inhibiting carrier loss to adjacent aqueous phases.  $\text{Sr}^{2+}$  transport varies linearly with membrane carrier concentration, suggesting a diffusion transport mechanism governed by the polarity and the viscosity of the plasticizer. It can be concluded that a membrane with a 37% CTA, 48% NPOE and 15% DtBuCH18C6 composition is very effective for the separation of  $\text{Sr}^{2+}$  in 1 M  $\text{HNO}_3$  + 2 M  $\text{NaNO}_3$ . The presence of  $\text{Al}(\text{NO}_3)_3$  enhances the transport of  $\text{Sr}^{2+}$ . The electivity of this PIM for  $\text{Sr}^{2+}$  over nuclides such as  $^{140}\text{La}$ ,  $^{96}\text{Nb}$ ,  $^{97}\text{Zr}$ ,  $^{99}\text{Mo}$ ,  $^{103}\text{Ru}$ ,  $^{143}\text{Ce}$  and  $^{151}\text{Pm}$  is excellent. The interference of  $^{140}\text{Ba}$  is explained on the basis of the close size match of  $\text{Ba}^{2+}$  and the cavity of the 18-membered ligand.

## References

- 1 Feasibility of separation and utilisation of caesium and strontium from high-level waste, Technical Report Series, International Atomic Energy Agency, Vienna, 1993, No. 356, p. 5.
- 2 W. W. Schulz and L. A. Bray, *Sep. Sci. Technol.*, 1987, **22**, 191.
- 3 E. P. Horwitz, M. L. Dietz and D. E. Fisher, *Solvent Extr. Ion Exch.*, 1990, **8**, 557.
- 4 E. P. Horwitz, M. L. Dietz and D. E. Fisher, *Solvent Extr. Ion Exch.*, 1991, **9**, 1.
- 5 E. P. Horwitz, M. L. Dietz and R. D. Rogers, *Solvent Extr. Ion Exch.*, 1995, **13**, 1.
- 6 A. Kumar, P. K. Mohapatra and V. K. Manchanda, *Radiochim. Acta.*, 1999, **85**, 113.
- 7 P. K. Mohapatra and V. K. Manchanda, *Indian J. Chem., Sect. A: Inorg., Bio-Inorg., Phys., Theor. Anal. Chem.*, 2003, **42**, 2925.
- 8 R. Chiarizia and E. P. Horwitz, *Solvent Extr. Ion Exch.*, 1990, **8**, 65.
- 9 M. G. Hankins and R. A. Bartsch, *Solvent Extr. Ion Exch.*, 1995, **13**, 983.
- 10 J. D. Lamb, R. L. Bruening, R. M. Izatt, Y. Hirashima, P. Tseand and J. J. Christensen, *J. Membr. Sci.*, 1988, **37**, 13.
- 11 M. Sugiura, *Sep. Sci. Technol.*, 1992, **27**, 269.
- 12 A. Kumar, P. K. Mohapatra, P. N. Pathak and V. K. Manchanda, in *Proceedings of Nuclear and Radiochemistry Symposium*, eds. K. L. Ramakumar, R. M. Kadam, V. N. Vaidya and D. S. C. Purushottam, Bhabha Atomic Research Centre, Trombay, Mumbai, 2001, p. 428, CFAP-21..
- 13 J. D. Lamb and A. Y. Nazarenko, *Sep. Sci. Technol.*, 1997, **32**, 2749.
- 14 A. J. Schow, R. T. Peterson and J. D. Lamb, *J. Membr. Sci.*, 1996, **11**, 291.
- 15 L. B. Kumbhare, D. R. Prabhu, G. R. Mahajan, S. Sriram, V. K. Manchanda and L. P. Badheka, *Nucl. Technol.*, 2002, **139**, 253.
- 16 Y. Takeda, *Top. Curr. Chem.*, 1984, **121**, 1.
- 17 J. F. Duzol, J. Casas and A. M. Sastre, *Sep. Sci. Technol.*, 1993, **28**, 2007.
- 18 D. W. McBride, Jr., R. M. Izatt, J. D. Lamb and J. J. Christensen, in *Inclusion Compounds III*, Academic Press, London, 1984, pp. 571–628.
- 19 J. A. Riggs and B. D. Smith, *J. Am. Chem. Soc.*, 1997, **119**, 2765.
- 20 M. L. Dietz, E. P. Horwitz and R. D. Rogers, *Solvent Extr. Ion Exch.*, 1990, **13**, 1.
- 21 A. Kumar, P. K. Mohapatra, P. N. Pathak and V. K. Manchanda, *Talanta*, 1997, **45**, 387.